Mid-Air Thermo-Tactile Feedback using Ultrasound Haptic Display

Yatharth Singhal
The University of Texas at Dallas
Richardson, TX, USA
Yatharth.Singhal@UTDallas.edu

Haokun Wang
The University of Texas at Dallas
Richardson, TX, USA
Haokun.Wang@UTDallas.edu

Hyunjae Gil
Ulsan National Institute of Science and Technology
Ulsan, Republic of Korea
hyunjaegil@gmail.com

Jin Ryong Kim
The University of Texas at Dallas
Richardson, TX, USA
Jin.Kim@UTDallas.edu

ABSTRACT

This paper presents a mid-air thermo-tactile feedback system using an ultrasound haptic display. We design a proof-of-concept thermo-tactile feedback system with an open-top chamber, heat modules, and an ultrasound display. Our approach is to provide heated airflow along the path to the focused pressure point created from the ultrasound display to generate thermal and vibrotactile cues in mid-air simultaneously. We confirm that our system can generate the thermo-tactile stimuli up to 54.2°C with 3.43 mN when the ultrasonic haptic signal was set to 100 Hz with a 12 mm radius of the cue size. We also confirm that our system can provide a stable temperature (mean error=0.25%). We measure the warm detection threshold (WDT) and the heat-pain detection threshold (HPDT). The results show that the mean WDT was 32.8°C (SD=1.12), and the mean HPDT was 44.6°C (SD=1.64), which are consistent with the contact-based thermal thresholds. We also found that the accuracy of haptic pattern identification is similar for non-thermal (98.1%) and thermal conditions (97.2%), showing a non-significant effect of high temperature. We finally confirmed that thermo-tactile feedback further enhances the user experiences.

CCS CONCEPTS

• **Human-centered computing** → **Haptic devices**; *Displays and imagers*; **User studies**; **Mixed / augmented reality**.

KEYWORDS

Mid-air haptic feedback, thermo-tactile feedback, thermal feedback

ACM Reference Format:
Yatharth Singhal, Haokun Wang, Hyunjae Gil, and Jin Ryong Kim. 2021. Mid-Air Thermo-Tactile Feedback using Ultrasound Haptic Display. In *27th ACM Symposium on Virtual Reality Software and Technology (VRST '21), December 8–10, 2021, Osaka, Japan.* ACM, New York, NY, USA, 11 pages. https://doi.org/10.1145/3489849.3489889

VRST '21, December 8–10, 2021, Osaka, Japan

ACM ISBN 978-1-4503-9092-7/21/12…$15.00
https://doi.org/10.1145/3489849.3489889

1 INTRODUCTION

Virtual Reality (VR) is on the rise. Designers, engineers, and researchers around the globe are working towards making the VR experience better and more immersive. Many VR applications incorporate surreal and realistic haptic feedback in addition to visual and auditory modalities for multimodal interaction. A large amount of emphasis is now put on providing thermal feedback in VR to increase the sense of immersion and presence. Just like a physical world, many VR scenarios require thermal feedback – people use hot water from the faucet, feel the fireplace's ambient temperature, or face falling snow in a winter scene.

It is known that thermal perception is based on the absolute and relative changes in skin temperature. That is, humans perceive warmth and coldness when their thermoreceptors respond to the stimulus that is above or below the skin temperature [6, 22]. This information is conveyed to the insula cortex (a region of the brain deep in the cerebral cortex) rather than the somatosensory cortex [5]. However, the exact mechanism of activation associated with skin temperature changes is still unknown.

Thermal feedback is used to enhance realism [23, 51], provide realistic perception of virtual objects [10, 26, 59], or used as an ambient communication channel [26, 44, 47, 48, 56, 57]. Many of the contact-based thermal feedback approaches incorporate the use of Peltier devices to provide thermal feedback [37–39, 48] while others use infrared lasers [34], infrared lamps [42], thermal radiation [45], liquid [14], or utilize other sensory perception like sight [55] or smell [3] to create an illusion of thermal sensations.

Providing thermal sensations in mid-air is important as free-hand interaction is a promising direction that provides more natural and intuitive interactions in the virtual environment. Several studies have focused on non-contact thermal and humidity feedback, and many of them have used thermal items like infrared lamps, heaters, fans, and projector lights. Hülsmann et al. [18] delivered wind and thermal feedback using IR lamps and fans to the interaction space. Han et al. [15] developed a system that delivers global thermal feedback by utilizing fans, lamps, mist, and heat light installed around the user. Shaw et al. [46] presented an IR heater system to generate global warm thermal feedback for fire evacuation scenarios. Iwai et al. [20] used an IR RGB projector light to provide a thermo-visual perception system in augmented reality. Nakajima et al. [35, 36] presented the methods to provide cold feedback using ultrasound-driven airflow. Xu et al. [58] proposed a method to present cold

sensations by passing the air through a vortex tube. However, due to their underlying mechanisms, all the approaches have the limitation that it's not easy to control the thermal cues in 3D space. Recently, Kamigaki et al. [24, 25] proposed a method using ultrasound display to create a focal point in mid-air on a hand-worn glove to provide thermal sensations. Their work is promising as an ultrasound mid-air haptic display is scalable and easy to control the vibrotactile cues' size and frequency in 3D space. However, their method requires a glove to feel the thermal feedback, which is not appropriate for bare-hand interaction.

Our method takes advantage of providing tactile and thermal cues simultaneously by integrating both vibrotactile stimulus created from ultrasound display and thermal stimulus from heated air created and kept in a chamber. Yet, it is not clear how simultaneous presentation of both stimuli is being processed and perceived as an individual signal; it is reported that the thermal feedback enhances the tactile sensory acuity (i.e., thermal sharpening) [49, 50]. It is also reported that the thermal identification rate in the warm stimulus is higher than that of cold stimulus (89% vs. 76%) [48] in thermo-tactile displays. Our method is based on the human ability to identify the tactile and thermal patterns without masking each other. We further leverage the underlying principles of ultrasound display that provides acoustic pressure at mid-air. By generating the heated air, we can create a heated pressure point to simultaneously present thermal and vibrotactile cues.

This paper proposes a proof-of-concept system that provides thermo-tactile feedback in mid-air using an ultrasound display with an open-top chamber and heat elements for bare-hand interaction. Mid-air ultrasound haptic technology is based on the algorithm that creates a focused pressure point in 3D space using multiple ultrasound speakers, and a significant amount of research has been carried out [4, 11, 16] with many applications [12, 19, 29, 60, 63]. We believe that we show one promising direction towards creating mid-air thermo-tactile feedback by considering human perception and utilizing underlying principles of ultrasound display.

2 IMPLEMENTATION

2.1 Design

Figure 1 shows the design of our proof-of-concept prototype. It consists of two heat modules, an ultrasound display, and an open-top chamber for retaining heat inside while allowing heat to flow upward. Inside each heat module, a ceramic heating element (JKFTP-120-250, Delonghi, China) is symmetrically placed at each side of the chamber (see Figure 2). Two fans are also placed behind each heating element to inflate heated airflow into the chamber. Each ceramic heating element circuit board is connected to a variable output autotransformer (TDGC2-0.5D, Variac, USA) to control the temperature by adjusting the input voltage to the heating element. The chamber is constructed using cardboard and then wrapped with aluminum foil to retain heat inside the chamber. The chamber has the shape of two conical frusta with a height of 100 mm connected by sharing a surface with a radius of 250 mm while having the other surface with a radius of 180 mm for the top and 150 mm for the bottom. The volume of the chamber is 0.274 m^3. The top is cut out in the shape of a circle with a radius of 150 mm. An ultrasonic haptic display (STRATOS Explore, Ultraleap, UK) is placed inside

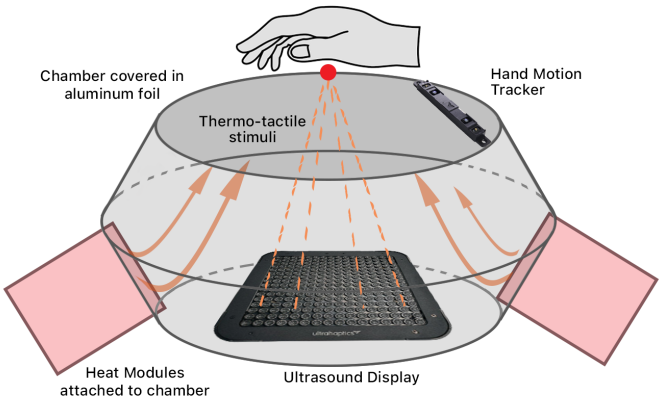

Figure 1: A concept of the proposed system

the chamber, facing upward. A hand tracking device (Stereo IR 170, Ultraleap, UK) is installed on the prototype's upper surface to track users' hands to deliver the thermo-tactile feedback to their hands. We adjusted the position of the hand-tracking device with the offset equal to the device's distance from the mid-point of the ultrasound array. We installed a digital thermometer (DS18B20, Maxim Integrated, Inc.) close to the ultrasound focal point above the chamber and another outside the setup to monitor the room temperature. The digital thermometer has a user-configurable resolution from 9 bits to 12 bits. In this work, the resolution was configured to 12 bits, yielding the accuracy of ±0.0625 °C. All the temperature data was monitored and recorded in real-time.

When both heating elements are activated by applying the voltage from the variable output autotransformers, the heating elements produce heat energy to heat and circulate air, and the fans speed up the airflow (i.e., fan heaters). The temperature of the airflow is controlled using autotransformers, which have an adjustment range from 0 V to 110V. The heater power is proportional to the square of supply voltage level. Thus, adjusting the transformer voltage would change the power of the heating element and result in different temperatures in the airflow. We kept the fan's speed at a constant 2000 revolutions per minute (RPM) after testing various values ranging from 1800 to 3500 RPM. We found that the RPM values lower than 2000 could not spread the heat evenly inside the chamber (monitored by placing two thermal sensors on the diagonally opposite end of the chamber). The higher values provided lower heat as the fans gave a cooling effect instead. Once the heated airflow is inflated into the chamber, the heated air is kept in the chamber. The chamber's temperature is increased as the heating elements increase the voltage (i.e., produce more heat energy) until it reaches a certain temperature in the chamber. The chamber's temperature can be decreased by lowering the voltage of the heating element.

When the ultrasound haptic display is activated, the focused ultrasonic haptic cues with different temperatures are created through the open-top of the chamber, passing through the heated air. In our

setup, a circular haptic cue with a radius of 12 mm is generated at 200 mm from the haptic display. Participants can interact with an apparatus by horizontally outstretching their hands in an open space between the apparatus's top surface and 100 mm above it, which we refer to as *interaction space*. Figure 2(b) shows thermal images of a participant's hand in the interaction space. The ultrasound display and the heaters (operated at 120V) were turned on and operated for 100 seconds, during which the thermal camera captured an image every 10 seconds for 100 seconds. The experiment was conducted in a room with an area of 600 square feet and a height of 9 feet. The room temperature was set to 23 °C throughout all experiments. The prototype was placed on a table adjusted to make it comfortable for participants to keep their hands in the interaction space while sitting on a chair.

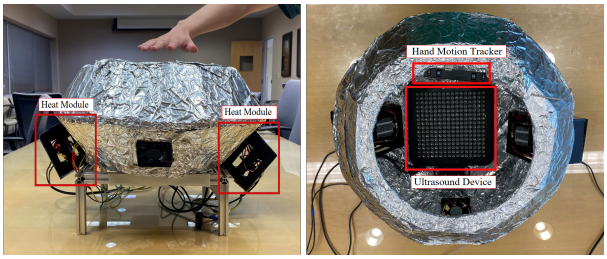

(a) Side and top view

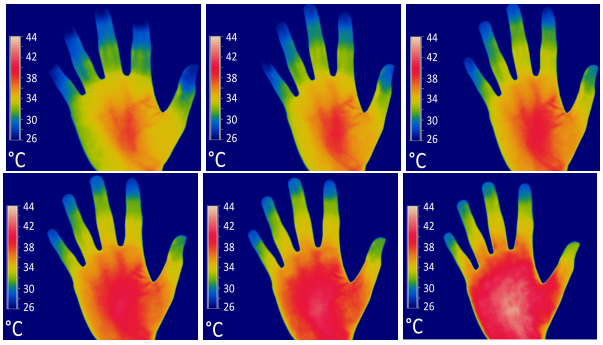

(b) Thermal camera images of the user's palm in 0, 10, 20, 40, 60, 100s

Figure 2: (a) A prototype system - top and side views and (b) thermal images showing affected area from t=0s to t=100s.

2.2 Simulation

Our prototype design was evaluated with the finite element simulation to validate the thermal process. Figure 3 shows the simulation model and the results of the proposed prototype system. We used the ANSYS workbench to simulate the heat flow and temperature distribution of the system. The model contains the same structure, components, and dimension as the proposed system (open-top chamber, two ceramic heaters with fans). The thermal simulation has been assessed with ANSYS Fluent with optimized boundary conditions based on physical properties of materials being used in the prototype. The rated heat source power was set to 250W and the fan was set to 2000 RPM. The model is meshed by body

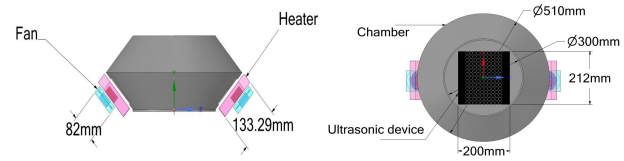

(a) Simulation model side and top view

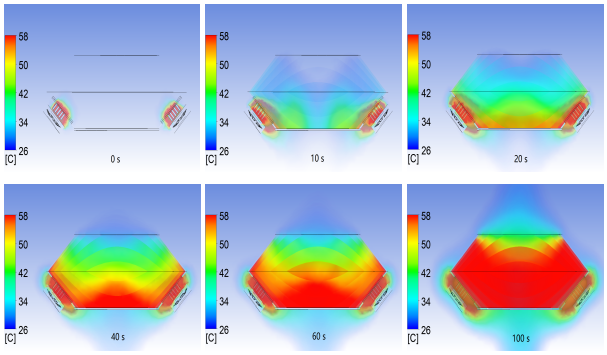

(b) Thermal simulation results in 0, 10, 20, 40, 60, 100s

Figure 3: Simulation model and its result (a) top and side view, (b) simulation results from t=0s to t=100s.

mesh with 2 mm and analyzed in fluid transient at a time step of 0.1 seconds. The total time of simulation was 100 seconds.

Table 1 shows materials and their physical characteristics applied in a simulation, such as density, specific heat capacity, and thermal conductivity. The results of temperature distribution at different timestamps are also shown in Figure 3. Based on our simulation result, the focal point temperature would rise to 25 °C from 22 °C in 10 seconds, which shows an efficient heat process considerably given the large chamber volume. After that, the temperature would rise to 28 °C in another 10 seconds. Then in the next 60 seconds, the temperature curve would follow linear growth and would raise 3.2 °C every 10s and reach 47 °C after 80 seconds. From the 80 seconds to 100 seconds, it showed that the temperature has some fluctuation but would maintain at least 44 °C. The simulation data shows that the system has a good heating process and can keep the high temperature in the proposed exposure time (7 seconds), which meets our design goal.

2.3 Impact of Thermal Process on Ultrasound Power Attenuation

We show the impact of the thermal effect on ultrasound power attenuation through mathematical deduction. We validate that if the ultrasound power attenuation remains the same level upon both the high and low-temperature conditions, then the thermal impact on mid-air haptic feedback is negligible. We first start with the entire thermal process from thermal generation on PTC (Positive Temperature Coefficient) heater to thermal receipt on hand contact region. We then discuss the impact of the thermal effect on ultrasound power attenuation.

Table 1: Material and their physical features

Component	Material	ρ (kg/m^3)	C (J/kg.K)	K (W/m.K)
Chamber surface cover	Aluminium	2710	0.897	239
Ceramic Heater	PTC ceramic	6060	527	6
Chamber support structure	Card board	689	1700	0.1
Fan and fan case	Polylactic Acid	1210	1800	0.13
Heater case	Acrylonitrile butadiene styrene	1070	1500	0.1

The heat source in this apparatus is a PTC heater, which has high efficiency and reliability, with a rated power of 110V (250W). The heat power can be expressed as equation below based on the PTC feature of variant resistant value in response to the temperature change:

$$P = \frac{V^2}{R_{PTC}} = \frac{T_{SPTC} - T_A}{R_{th}} \tag{1}$$

where V denotes the rated voltage, R_{PTC} denotes the PTC heater resistance, T_{SPTC} denotes the surface temperature of PTC heater, T_A denotes the ambient temperature, and R_{th} denotes the thermal resistance [31].

The generated heat is then transferred to the chamber through the fan air fluid flow. Although radiation exists, based on the low radiation temperature (not exceed 120° in rated power), thermal convection is the main way of heat transfer and can be written as

$$Q_{conv} = hA(T_{SPTC} - T_A) \tag{2}$$

where Q_{conv} denotes the convective heat transfer rate between PTC heater and air. Here, h denotes heat transfer coefficient and is composed of two parts:

$$h = h_n + h_f \tag{3}$$

where h_n denotes the natural convection coefficient and h_f denotes the forced convection coefficient due to temperature difference and fluid flow, respectively. Then the hot air would heat the hand skin to implement the thermal sensation:

$$Q_f = m_f C_p (T_A - T_S) \tag{4}$$

where Q_f denotes the rate of heat transfer, m_f denotes the air mass flow rate, and C_p denotes the specific heat of air [21]. The air mass flow rate is:

$$m_f = \rho_a v_a A \tag{5}$$

where v_a denotes the air velocity. Given the hot air flow and chamber structure, the air velocity and viscosity are vary across space, which would impact the sound pressure level [40]. However, based on calculation and test these influences to mid-air haptic feedback are trivial.

The general expression for the velocity of sound in gases under standard conditions is:

$$v = (\frac{\gamma P}{\rho})^{0.5} \tag{6}$$

where γ is the ratio of the specific heats of the gas (1.414 in case of air), P is the pressure (101,325 Pa), and ρ is the density of the gas (1.225 kg/m3). Increasing pressure will increase the density in the same proportion. Under constant temperature conditions, the velocity v is independent of pressure [8]. Thus, the relationship between sound velocity and temperature can be expressed as:

$$v = 331 + 0.6t \tag{7}$$

where t denotes the temperature in degree Celsius (°C). The attenuation is the term used to account for the loss of wave amplitude due to all mechanisms (i.e., absorption, scattering, mode conversion, etc.) and is shown as:

$$A = A_0 e^{-\alpha z} \tag{8}$$

where A_0 denotes the unattenuated amplitude, z denotes the distance, α is the attenuation coefficient which can be expressed below based on Stokes's law of sound attenuation:

$$\alpha = \frac{2\mu\omega^2}{3\rho v^3} \tag{9}$$

where μ is the dynamic viscosity of the fluid, ω is the sound's angular frequency, ρ is the fluid density, and v is the speed of sound in the medium [17]. Under this experiment condition, the temperature range in the chamber between 25°C (i.e., room temperature) and 45°C (i.e., hot temperature), and result in a sound pressure level change of 1.07%, which can be neglected [13].

From the mathematical deduction shown above, it can be concluded that the thermal impact on ultrasound power attenuation is trivial, and the proposed system could provide thermal feedback while not interrupting the mid-air vibrotactile sensation.

2.4 System Characteristics

Figure 4 shows the temperature changes in interaction space at each voltage level, ranging from 60V to 120V with a step size of 10V. We adjusted both autotransformers to one of the voltage levels and recorded the temperature changes for 300 seconds. We found that the maximum temperature that the system can achieve after 300 seconds was 54.2 °C at 120V, which is close to the simulation result of 56.6 °C and is within the range of acceptable error. It was also observed that there are considerable temperature differences in the final temperature when applied voltages are less than 100V. Still, the differences become relatively smaller when it is 100V or larger. The difference between 120V and 110V was minuscule (1.6 °C).

At each level, the temperature was adjusted and maintained for seven seconds. This measurement was repeated ten times for each temperature level, yielding 70 seconds in total. We then averaged them and calculated each temperature level's variation and corresponding error rates. The mean variation was 0.09°C (SD=0.02), and the mean error rate was 0.25% (SD=0.07), confirming stable temperature at each level.

3 EXPERIMENT 1: MEASURING THERMO-TACTILE THRESHOLDS

This experiment aims to estimate the mid-air thermo-tactile thresholds at which users can detect the warm stimulus and heat-pain stimulus when the focused ultrasound haptic feedback is delivered to the user's palm. The warm detection threshold (WDT) can be described as the temperature at which the users can start perceiving

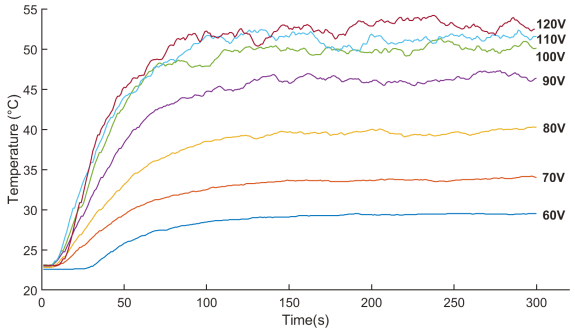

Figure 4: Target temperature changes over time at each voltage level, ranging from 60V to 120V with a step size of 10V.

warm sensations, whereas the heat-pain detection threshold (HPDT) is a point along the curve of increasing perception of thermal stimuli at which pain begins to be felt [7, 52]. Perception thresholds for heat in contact-based thermal stimuli are ranged from 32.5°C to 36.7°C for WDT and from 43.0°C to 46.8°C for HPDT, respectively [2, 27, 30, 61].

3.1 Participants

Twelve participants, ranging from 22 to 29 years old (4 females; mean: 25.25 years old, std. dev. 2.2 years old) took part in the experiment. All participants were right-handed. None of them reported any disorder affecting the sensations of their hands. Each participant was paid with a $10 gift card for their participation. All the participants gave written informed consent to participate in the study. All the experiments were approved by the Institutional Review Board (IRB) of the University of Texas at Dallas (IRB-21-194).

3.2 Apparatus

We used our prototype system as an apparatus for this experiment. As we mentioned in the previous section, circular haptic feedback with a radius of 12 mm is generated at 100 Hz with 1.0 intensity (3.43 mN) [43]. We considered the trade-off between the stronger perceived intensity of 200 Hz and its audible noise that may degrade the user experience. We decided to set 100 Hz of ultrasound signal as a fair trade-off.

3.3 Experimental Design

We used a psychophysical method called a "simple one-up and one-down staircase method" that adapts to the participant's threshold level [32, 33] with an estimation of the 50% point of the psychometric function [41] for both WDT and HPDT. Each threshold was measured twice for each participant. We measured WDT, followed by HPDT. The threshold was estimated by averaging six reversals in each repetition.

3.4 Procedure

Instructions were given to each participant with a short description of our prototype and the procedure before the main experiment. The participant was asked to place their dominant hand on top of the chamber for seven seconds and then answer a Yes/No question on each trial. We chose seven seconds of exposure time based on the initial observation from a pilot study with three different exposure time values (i.e., 5s, 7s, and 10s). We found that exposing the hand for five seconds was too short to feel, and exposing it for ten seconds may result in experiencing slight burning sensations at high temperatures. After exposing their palm for seven seconds, participants were required to answer either "Yes" or "No," depending on whether they felt thermal sensations. For WDT measurement, they were required to respond with "Yes" if the sensation was *warm* and respond with "No" otherwise. For HPDT measurement, they were required to respond with "Yes" if the sensation was *hot and discomforting* and respond with "No" otherwise. The experimenter then entered this response on a computer. We decided the experimenter should record responses instead of the participants to ensure proper health precautions were taken, and no equipment was being shared. This was a forced-choice paradigm, and the participants were required to guess if they were not sure of their response. The starting temperature for WDT and HPDT were 28.0°C and 36.0°C, respectively. These initial temperatures were obtained based on baseline temperatures reported in [1], and we confirmed it through our pilot study.

We adjusted the temperature by a step-size of 1°C based on the response from the participant. If they respond with "Yes", the temperature is decreased by a step-size of 1°C. If they answer "No," the temperature is increased by a step-size of 1°C. This was continued until they changed their answer (i.e., reversal). We increased the step-size to 2°C at the beginning of the trials until it reached the first reversal to converge to the expected threshold quickly, and we kept the step-size to 1°C for the rest of the trials to secure the resolution of the estimated threshold. The experiment is continued until six reversals are reached. The six reversals are then averaged for an estimated threshold. The duration of the experiment was typically 80 minutes, and participants were asked to take a 5-minute break between repetitions.

3.5 Results and Discussion

Figure 5 shows typical series of trials with an estimated threshold for one participant (P9). Figure 5(a) shows a trial for WDT and Figure 5(b) shows a trial for HPDT. The black square represents positive response ("Yes"), and the white circle represents negative response ("No"), respectively. As we described in the procedure, we increased the step size to 2°C until it reached the first reversal (R_1), then we changed to 1°C for the rest of the trials. The mean of all the reversals (R_1-R_6) is taken to calculate the participant's estimated threshold.

The mean WDT was 32.8°C (SD=1.12), and the mean HPDT was 44.6°C (SD=1.64). These values were congruous to the findings from contact-based warm perception and heat pain thresholds [2, 27, 30, 61]. We confirmed that WDT and HPDT remained the same at room temperature.

4 EXPERIMENT 2: PATTERN IDENTIFICATION

This experiment investigates the impact of thermal conditions on the ability to identify vibrotactile patterns presented in mid-air. As we proved no significant impact of the thermal conditions on

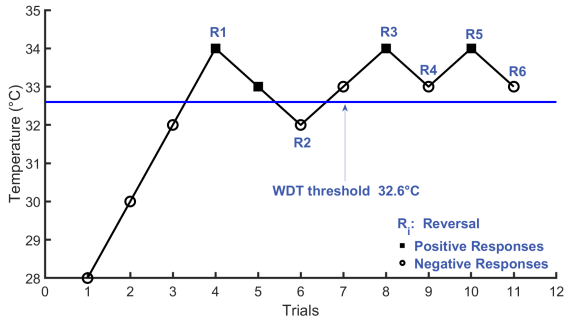

(a) WDT

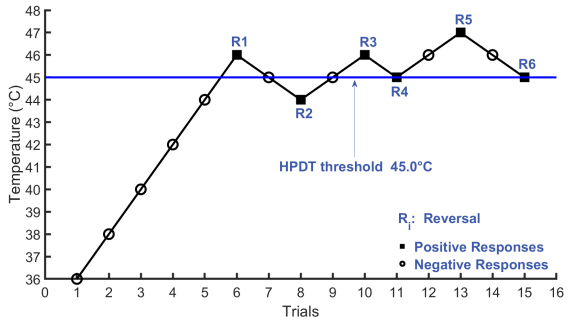

(b) HPDT

Figure 5: A typical series of trials from one participant (P9): (a) WDT and (b) HPDT.

mid-air haptic feedback through mathematical deduction, we also want to verify it through this user experiment.

4.1 Participants

Twelve participants who did not participate in Experiment 1 were recruited to participate in this experiment (3 females; mean age = 24.2 years old; SD = 4.28). All participants were right-handed, and none of them reported any disorder affecting the sensations of their hands. Each participant was paid a $10 gift card for their participation. All the participants gave written informed consent to participate in the study.

4.2 Apparatus

Our prototype system was used as an apparatus for this experiment. In addition, we prepared another set of ultrasound displays (without heat modules and chamber) that was identical to the prototype system for non-thermal conditions. The haptic feedback was generated at 100 Hz with 1.0 intensity for all feedback patterns.

4.3 Experimental Design

We designed a within-subject with three tasks (*TaskPoint*, *TaskShape*, *TaskMove*), with each task focused on different types of haptic patterns in mid-air using two thermal conditions: i) non-thermal condition at 23°C (room temperature) and ii) thermal condition at 44°C (chosen based on *HPDT* from experiment 1). All three tasks were designed to present mid-air haptic feedback on the palm of the user's dominant hand.

TaskPoint. This task was designed to investigate if the thermal stimulus had any effects on identifying multiple points in mid-air (see Figure 6(a)). There are three patterns, with each having a vibrotactile point with a radius of 12 mm: i) a single point presented on the center of the palm, ii) two vibrotactile feedback points placed 4 cm apart in the longitudinal direction, and iii) four vibrotactile points with each placed on the vertices of a square with a length of 4 cm. The total number of trials was 60 (3 haptic patterns × 2 thermal conditions × 10 repetitions). The order of tasks as well as the order of trials within tasks were randomized and counterbalanced by using the Latin squares method.

TaskShape. This task compares thermal and non-thermal conditions when different types of two-dimensional vibrotactile shapes were presented on the user's palm in mid-air. Figure 6(b) shows the visual representations of patterns: i) a solid line with a length of 4 cm, ii) a square with its edge length of 4 cm, and iii) a circle with its diameter of 4 cm. Similarly, the total number of trials was 60 (3 haptic patterns × 2 thermal conditions × 10 repetitions).

TaskMove. This task comprised a 12 mm radius of vibrotactile feedback that moves from the center of the palm to one of the four directions (i.e., forward, backward, right, and left) with a speed of 4 cm per second, yielding the total travel distance of 4 cm (see Figure 6(c)). In each trial, the direction movement was presented three times with an interval of 200 ms. Thus, the total number of trials was 80 (4 haptic patterns × 2 thermal conditions × 10 repetitions).

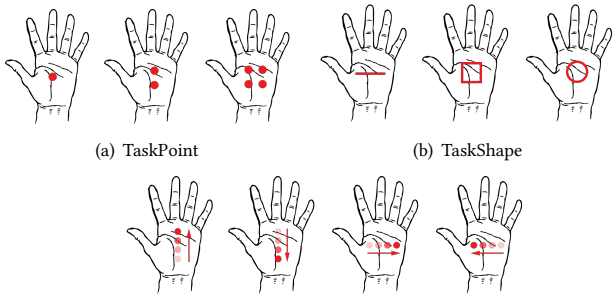

(a) TaskPoint (b) TaskShape

(c) TaskMove

Figure 6: Diagram illustrating the sensation felt for different Tasks. (a) TaskPoint, (b) TaskShape, and (c) TaskMove.

4.4 Procedure

Participants were briefed about the experiment procedure and asked to read and sign a consent form. At the beginning of each task, participants were asked to participate in a practice session to familiarize themselves with different vibrotactile patterns presented in each task. After each practice session, participants were asked to place their dominant hand on top of the apparatus while perceiving different combinations of haptic patterns. Depending on the thermal conditions, they experimented using our prototype system for thermal conditions and an identical ultrasound haptic display (without thermal components) for non-thermal conditions.

Each trial lasted for 10 seconds, and participants were asked to answer which pattern they perceived through their palms. The experimenter then recorded their response on a computer. Each task took approximately 15 minutes, and a 5-minute break was given between tasks. The entire experiment lasted 60 minutes, including the time to fill out the questionnaire.

4.5 Results and Discussion

Figure 7 shows the normalized confusion matrices presenting the mean vibrotactile pattern identification accuracy across participants for all three tasks in both conditions. The top confusion matrices (shown in blue) denote the non-thermal condition, and the bottom (shown in red) denotes the thermal condition. The mean identification accuracy was 98.1% (non-thermal) and 97.2% (thermal), respectively. It was also found that solid two dimensional shapes are slightly difficult to identify (mean accuracy of *TaskShape* = 94.58%) as compared to multiple vibrotactile point sensations (mean accuracy of *TaskPoint* = 98.05%) and animated vibrotactile sensations (mean accuracy of *TaskMove* = 98.56%). We confirmed that the difference of thermal condition was not significant across all tasks (p=0.10243 for *TaskPoint*; p=0.40687 for *TaskShape*, and p=0.128377 for *TaskMove*), demonstrating that vibrotactile patterns presented in mid-air are clearly perceivable with a high accuracy rate in a high temperature condition.

5 EXPERIMENT 3: VR APPLICATIONS

This experiment investigates the effect of thermo-tactile feedback in VR applications by comparing it with other modalities. We designed two VR scenes with four haptic feedback conditions while providing immersive VR scenes with visuals and audio feedback.

5.1 Participants

Sixteen participants who are not overlapping with either of the previous experiments took part in this experiment (3 females; mean age = 25.6 years old; SD=2.08). One participant was left-handed, and the rest of them were right-handed. None of them reported any disorder affecting the sensations of their hands. Each participant was paid with a $10 gift card for their participation. All participants gave written informed consent to participate in the study.

5.2 Apparatus

An Oculus Quest 2 VR headset was used along with our prototype system. The headset was connected to the main system (Lenovo Legion 5 with GeForce RTX 2060, Intel i7 1070H, and 16GB RAM) to run the VR applications developed using Unity 3D. Noise cancellation headphone was used to play pertinent audio cues and block out exterior noise.

5.3 Experimental Design

A within-subject experiment focusing on four haptic feedback conditions was conducted: i) *No Feedback*, ii) *Tactile Feedback*, iii) *Thermal Feedback*, and iv) *Thermo-Tactile Feedback*. *No Feedback* is a condition that does not provide any haptic feedback. In this feedback condition, there was no mid-air haptic feedback or thermal feedback presented. In *Tactile Feedback*, only ultrasound mid-air haptic feedback was presented without activating the thermal feedback.

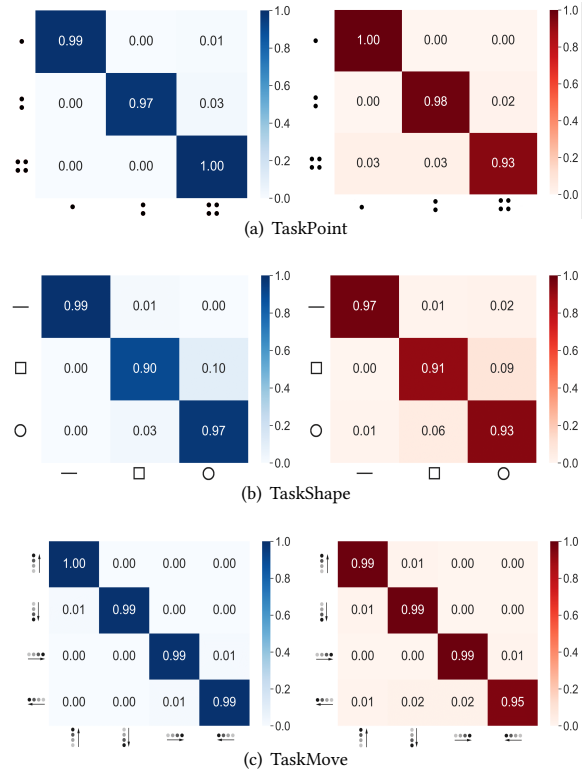

Figure 7: Normalized confusion matrices showing mean identification accuracy across the participants for (a) TaskPoint, (b) TaskShape, and (c) TaskMove. Blue shows the non-thermal condition, and red shows the thermal condition.

In *Thermal Feedback*, only thermal feedback was presented without providing ultrasound mid-air haptic feedback. Finally, *Thermo-Tactile Feedback* provided both ultrasound mid-air haptic feedback and thermal feedback. We designed two virtual scenes – *CampFire* and *WaterFountain*. A scene was arbitrarily selected to start the experiment, and feedback conditions within the scene were randomized and counterbalanced using Latin Square. All the appropriate visual scenes with animation and sound effects were provided in all feedback conditions.

CampFire: Figure 8(a) shows the campfire scene. In this scene, the user interacts with the fire embers and smoke rising from the fire with their virtual hands. For *Tactile Feedback* and *Thermo-Tactile Feedback*, an ultrasonic cue with 100 Hz and 0.7 intensity was provided for 500 ms whenever an ember collided with the virtual hands. The temperature was set to 44°C to maximize the heat effect without reaching the pain threshold to resemble the fire. A crackling fire sound was also played along with the virtual scene to enhance the user experience.

Water Fountain: In this scene, a hot water fountain with a water stream coming out from the fountain was presented in a park (see Figure 8(b)). When the water stream collided with the user's hands, the height of the water stream was dynamically adjusted depending on the hand's position with the water splash. For *Tactile Feedback*

and *Thermo-Tactile Feedback*, a continuous circular haptic sensation having a radius of 4 cm with a frequency of 100 Hz and intensity of 1.0 was presented to the user's palm. A temperature of 38°C was chosen to emulate the feel of warm water hitting the palm. Audio feedback with water-flowing sound was provided through all conditions.

Questionnaire sheets were prepared to measure the participants' responses for their interaction experiences in three areas: *Immersion* – The feedback condition was immersive, and it kept me engaged while interacting with the scene; *Enjoyment* – I enjoyed interacting with the scene in this feedback condition; *Overall Satisfaction* – I felt that the feedback condition was satisfying. Participants were asked to respond to each question by marking a check on a horizontal line (visual analog scale) with a label on each end: 'Strongly Disagree' and 'Strongly Agree' per feedback condition.

(a) Campfire Scene

(b) Water Fountain Scene

Figure 8: Users' point of view while interacting with a) Campfire Scene and b) Water Fountain Scene.

5.4 Procedure

Instructions were given to each participant with a short training session to become familiarized with the device and the scenes before the main experiment. The main experiment consisted of two scenes: Campfire and Water Fountain. For each scene, a total of four feedback conditions were presented: *No Feedback*, *Tactile Feedback*, *Thermal Feedback*, and *Thermo-Tactile Feedback*. After each scene, participants were asked to fill out the questionnaire. A 5-minute break was provided between two scenes. The entire experiment took 30 minutes per participant.

5.5 Results and Discussion

Participants' continuous-scale ratings for the three measures were collected and linearly scaled from 0 to 100 (0: Strongly Disagree, 100: Strongly Agree). The mean scores and standard error are shown in Figure 9. *Thermo-Tactile Feedback* condition was clearly the preferred feedback in all measures in both scenes, while users prefer *Tactile Feedback* and *Thermal Feedback* less. *No Feedback* was the least preferred condition.

A two-way ANOVA with repeated measures was conducted to evaluate our collected data. Results showed a highly significant effect on conditions (p<0.001) in all three measures. Post-hoc comparison using Tukey test revealed that *No Feedback* and *Thermo-Tactile Feedback* showed a significant difference (p<0.001) for all three measures. We also confirmed that there was a significant difference between *Tactile Feedback* and *Thermo-Tactile Feedback* (p=0.001) and also between *Thermal Feedback* and *Thermo-Tactile Feedback* (p=0.006) for all three measures. There was no significant difference between *Thermal Feedback* and *Tactile Feedback* (p=0.83).

The results indicated that virtual experience can be significantly enhanced when thermal and vibrotactile cues are coupled together (*Thermo-Tactile Feedback* condition; mean rating: *No Feedback* = 0.53, *Tactile Feedback* = 0.73, *Thermal Feedback* = 0.74, *Thermo-Tactile Feedback* = 0.91). The results also revealed that participants preferred all the other conditions to the *No Feedback* condition.

6 GENERAL DISCUSSION

This study presented a proof-of-concept system that provides thermo-tactile feedback using an ultrasonic mid-air haptic display. We hypothesized that we could simultaneously present thermal and tactile cues by generating a heated pressure point in the 3D space using an ultrasound display, heat elements, and a chamber. The result of system characteristics confirmed that our system could generate the thermo-tactile stimuli up to 54.2°C with 3.43 mN at 100 Hz (radius: 12 mm). The system can provide a reasonably constant temperature at each temperature level (mean =0.09°C; SD=0.02). We further confirmed our hypothesis by conducting a series of user experiments. Overall, our proof-of-concept system showed the feasibility of delivering thermo-tactile feedback in mid-air.

We discovered that the perception thresholds in mid-air are consistent with contact-based detection thresholds. The mean was 32.8°C (SD=1.12) for WDT and 44.6°C (SD=1.64) for HPDT, respectively. These thresholds can be compared with the contact-based thermal thresholds reported in previous studies [2, 27, 30, 61], which are ranged from 32.5 to 36.7°C for WDT and 43.0 to 46.8°C for HPDT. We believe that our report on the thermal threshold on a human's hand is the first measure in mid-air to the best of our knowledge. We also confirmed that there was no thermal effect on identifying different vibrotactile patterns presented in mid-air. The overall mean identification accuracy in high temperature (44°C) was 97.2%, and we couldn't find any evidence of a thermal effect. We confirmed that the users were able to identify the different number of points (*TaskPoint*), types of shapes (*TaskShape*), and moving directions (*TaskMove*) with a high accuracy rate, and the results are similar to those in non-thermal conditions (23°C; mean accuracy=98.1%).

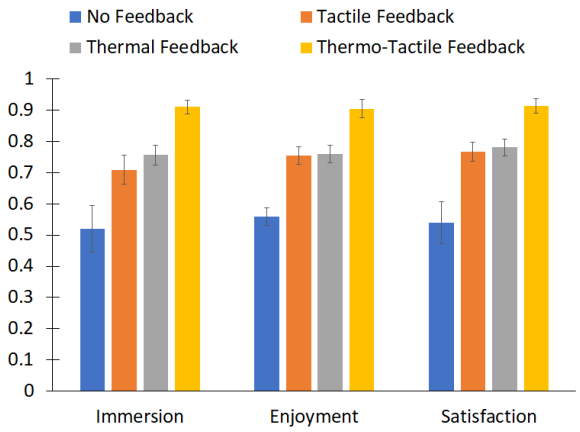

(a) Campfire Scene

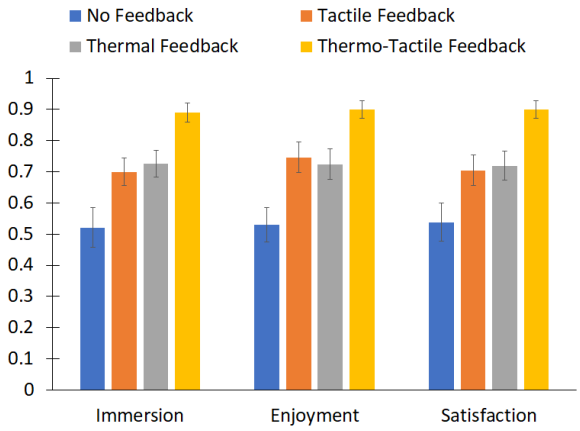

(b) Water Fountain Scene

Figure 9: Mean scores and standard error of all the measures in different feedback conditions for a) Campfire Scene and b) Water Fountain Scene based on participants' ratings.

One of the interesting findings in our study is the effects of thermo-tactile feedback on VR applications. We compared thermo-tactile feedback with other conditions to investigate how it can affect the user experiences in VR. We clearly observed the combinatory effect on the user experience when two modalities are combined (thermal + vibrotactile). We believe this is probably because users' expectations for sensations are satisfied with the combinatory effect of thermo-tactile feedback, yielding higher immersive VR experiences. In our experiment, the thermo-tactile feedback was directly mapped with the visual representations, and thus, we believe this is why we achieved a higher immersion for thermo-tactile feedback. The results are promising as users had a better user experience with thermo-tactile feedback than those with thermal only, tactile only, or no feedback. Some participants commented that they felt more natural and immersive with thermo-tactile feedback conditions because the feedback matches visual scenes.

Our proof-of-concept prototype system showed feasibility in delivering thermo-tactile feedback in 3D space. Because the prototype is based on ultrasound display technology, the users can feel the thermo-tactile feedback with various sizes and frequencies in mid-air. However, we also see room for improvement to be used as real-world applications. It is difficult to reach a certain temperature level within a short period, so that heating up to a certain temperature level takes a considerable time (see Figure 4). Still, the time interval from one temperature level to another is faster than the initial heat-up time; decreasing temperature levels take much longer than increasing temperature levels. Therefore, more precise and adaptive temperature control and cooling mechanism are required to improve this.

Furthermore, this work only considered providing feedback in an upward direction. In fact, there is no limit to the direction of providing mid-air thermo-tactile feedback, and it can deliver the sensations from any angle with minor changes in the setup. We believe that various applications can benefit from this flexibility if the feedback can be delivered from any angle. Moreover, studying the effects of temperature sensitivity of the skin with age on WDT and HPDT can be an interesting study to extend if the findings are different from contact-based thermo-tactile feedback [28, 62]. We also see that feedback strength is an important factor. Previous literature showed that various methods could improve vibrotactile intensity in mid-air [9, 53, 54], and this needs to be explored to improve the perceived intensity of the mid-air thermo-tactile feedback.

The present study shows one direction toward mid-air thermo-tactile feedback that can impact many application domains, from games and entertainment to education and training. As bare-hand interaction is extensively used in VR and AR as a promising interaction tool, providing thermo-tactile feedback to the bare hands in mid-air will bring another level of user experience. Our initial study showed a proof-of-concept system for delivering mid-air thermo-tactile feedback and validated its effectiveness through a series of user experiments. Overall, this study clearly showed that our system using mid-air thermo-tactile feedback could enhance the user experience, leading to greater immersion, enjoyment, and satisfaction.

7 CONCLUSION

We presented a mid-air thermo-tactile feedback system using an ultrasound haptic display with an open-top chamber. We confirmed that our proof-of-concept system could generate thermal and ultrasonic vibration feedback at the same time. We measured the thermal detection thresholds in mid-air and found that the mean WDT was 32.8°C and the mean HPDT was 44.6°C, respectively. We also confirmed that high thermal conditions do not significantly affect identifying different types of haptic patterns in mid-air. We finally demonstrated how thermo-tactile feedback affects the user experience in VR.

ACKNOWLEDGMENTS

We would like to thank Nicolas Chevrie, Henry Kim, Anjelica Avorque, and Yiqun Lu for their efforts in designing and developing VR scenes.

REFERENCES

[1] Mayienne Bakkers, Catharina G Faber, Martine JH Peters, Jos PH Reulen, Hessel Franssen, Tanya Z Fischer, and Ingemar SJ Merkies. 2013. Temperature threshold testing: a systematic review. *Journal of the Peripheral Nervous System* 18, 1 (2013), 7–18.

[2] Gillian Bartlett, John D Stewart, Robyn Tamblyn, and Michal Abrahamowicz. 1998. Normal distributions of thermal and vibration sensory thresholds. *Muscle & Nerve: Official Journal of the American Association of Electrodiagnostic Medicine* 21, 3 (1998), 367–374.

[3] Jas Brooks, Steven Nagels, and Pedro Lopes. 2020. Trigeminal-based Temperature Illusions. In *Proceedings of the 2020 CHI Conference on Human Factors in Computing Systems*. 1–12.

[4] Tom Carter, Sue Ann Seah, Benjamin Long, Bruce Drinkwater, and Sriram Subramanian. 2013. UltraHaptics: multi-point mid-air haptic feedback for touch surfaces. In *Proceedings of the 26th annual ACM symposium on User interface software and technology*. 505–514.

[5] Arthur D Craig, Kewei Chen, D Bandy, and Eric M Reiman. 2000. Thermosensory activation of insular cortex. *Nature neuroscience* 3, 2 (2000), 184–190.

[6] Ian Darian-Smith and Kenneth O Johnson. 1977. Thermal sensibility and thermoreceptors. *Journal of Investigative Dermatology* 69, 1 (1977), 146–153.

[7] Peter James Dyck, I Zimmerman, DA Gillen, D Johnson, JL Karnes, and PC O'Brien. 1993. Cool, warm, and heat-pain detection thresholds: testing methods and inferences about anatomic distribution of receptors. *Neurology* 43, 8 (1993), 1500–1500.

[8] F. Alton Everest. 2001. *The Master Handbook of Acoustics*. McGraw-Hill.

[9] William Frier, Damien Ablart, Jamie Chilles, Benjamin Long, Marcello Giordano, Marianna Obrist, and Sriram Subramanian. 2018. Using spatiotemporal modulation to draw tactile patterns in mid-air. In *International Conference on Human Haptic Sensing and Touch Enabled Computer Applications*. Springer, 270–281.

[10] Simon Gallo, Lucian Cucu, Nicolas Thevenaz, Ali Sengül, and Hannes Bleuler. 2014. Design and control of a novel thermo-tactile multimodal display. In *2014 IEEE Haptics Symposium (Haptics)*. Ieee, 75–81.

[11] LR Gavrilov and EM Tsirulnikov. 2012. Focused ultrasound as a tool to input sensory information to humans. *Acoustical Physics* 58, 1 (2012), 1–21.

[12] Hyunjae Gil, Hyungki Son, Jin Ryong Kim, and Ian Oakley. 2018. Whiskers: Exploring the use of ultrasonic haptic cues on the face. In *Proceedings of the 2018 CHI Conference on Human Factors in Computing Systems*. 1–13.

[13] Barry G Green. 1977. The effect of skin temperature on vibrotactile sensitivity. *Perception & Psychophysics* 21, 3 (1977), 243–248.

[14] Sebastian Günther, Florian Müller, Dominik Schön, Omar Elmoghazy, Max Mühlhäuser, and Martin Schmitz. 2020. Therminator: Understanding the Interdependency of Visual and On-Body Thermal Feedback in Virtual Reality. In *Proceedings of the 2020 CHI Conference on Human Factors in Computing Systems*. 1–14.

[15] Ping-Hsuan Han, Yang-Sheng Chen, Kong-Chang Lee, Hao-Cheng Wang, Chiao-En Hsieh, Jui-Chun Hsiao, Chien-Hsing Chou, and Yi-Ping Hung. 2018. Haptic around: multiple tactile sensations for immersive environment and interaction in virtual reality. In *Proceedings of the 24th ACM symposium on virtual reality software and technology*. 1–10.

[16] Keisuke Hasegawa and Hiroyuki Shinoda. 2013. A method for distribution control of aerial ultrasound radiation pressure for remote vibrotactile display. In *The SICE Annual Conference 2013*. IEEE, 223–228.

[17] Sverre Holm. 2019. *Waves with Power-Law Attenuation*. Springer.

[18] Felix Hülsmann, Julia Fröhlich, Nikita Mattar, and Ipke Wachsmuth. 2014. Wind and warmth in virtual reality: implementation and evaluation. In *Proceedings of the 2014 Virtual Reality International Conference*. 1–8.

[19] Inwook Hwang, Hyungki Son, and Jin Ryong Kim. 2017. AirPiano: Enhancing music playing experience in virtual reality with mid-air haptic feedback. In *2017 IEEE World Haptics Conference (WHC)*. IEEE, 213–218.

[20] Daisuke Iwai, Mei Aoki, and Kosuke Sato. 2018. Non-contact thermo-visual augmentation by IR-RGB projection. *IEEE transactions on visualization and computer graphics* 25, 4 (2018), 1707–1716.

[21] David G. Foster James Welty, Gregory L. Rorrer. 2019. *Fundamentals of Momentum, Heat, and Mass Transfer*. Wiley.

[22] Lynette A Jones and Hsin-Ni Ho. 2008. Warm or cool, large or small? The challenge of thermal displays. *IEEE Transactions on Haptics* 1, 1 (2008), 53–70.

[23] Lynette A Jones and Susan J Lederman. 2006. *Human hand function*. Oxford university press.

[24] Takaaki Kamigaki, Shun Suzuki, and Hiroyuki Shinoda. 2020. Mid-air Thermal Display via High-intensity Ultrasound. In *SIGGRAPH Asia 2020 Emerging Technologies*. 1–2.

[25] Takaaki Kamigaki, Shun Suzuki, and Hiroyuki Shinoda. 2020. Noncontact Thermal and Vibrotactile Display Using Focused Airborne Ultrasound. In *International Conference on Human Haptic Sensing and Touch Enabled Computer Applications*. Springer, 271–278.

[26] Peter Kammermeier, Alexander Kron, Jens Hoogen, and Günther Schmidt. 2004. Display of holistic haptic sensations by combined tactile and kinesthetic feedback. *Presence: Teleoperators & Virtual Environments* 13, 1 (2004), 1–15.

[27] Kiesa Getz Kelly, Thomas Cook, and Misha-Miroslav Backonja. 2005. Pain ratings at the thresholds are necessary for interpretation of quantitative sensory testing. *Muscle & Nerve: Official Journal of the American Association of Electrodiagnostic Medicine* 32, 2 (2005), 179–184.

[28] Marius A Kemler, Hubert JA Schouten, and Richard H Gracely. 2000. Diagnosing sensory abnormalities with either normal values or values from contralateral skin: comparison of two approaches in complex regional pain syndrome I. *The Journal of the American Society of Anesthesiologists* 93, 3 (2000), 718–727.

[29] Jin Ryong Kim, Stephanie Chan, Xiangchao Huang, Kenneth Ng, Limin Paul Fu, and Chen Zhao. 2019. Demonstration of refinity: an interactive holographic signage for new retail shopping experience. In *Extended Abstracts of the 2019 CHI Conference on Human Factors in Computing Systems*. 1–4.

[30] Alyssa K Kosturakis, Zijing He, Yan Li, Jessica A Boyette-Davis, Nina Shah, Sheeba K Thomas, Haijun Zhang, Elisabeth G Vichaya, Xin Shelley Wang, Gwen Wendelschafer-Crabb, et al. 2014. Subclinical peripheral neuropathy in patients with multiple myeloma before chemotherapy is correlated with decreased fingertip innervation density. *Journal of Clinical Oncology* 32, 28 (2014), 3156.

[31] Clemens JM Lasance. 2008. Ten years of boundary-condition-independent compact thermal modeling of electronic parts: A review. *Heat Transfer Engineering* 29, 2 (2008), 149–168.

[32] Marjorie R Leek. 2001. Adaptive procedures in psychophysical research. *Perception & psychophysics* 63, 8 (2001), 1279–1292.

[33] HCCH Levitt. 1971. Transformed up-down methods in psychoacoustics. *The Journal of the Acoustical society of America* 49, 2B (1971), 467–477.

[34] Richard A Meyer, Ronald E Walker, and Vernon B Mountcastle. 1976. A laser stimulator for the study of cutaneous thermal and pain sensations. *IEEE transactions on biomedical engineering* 1 (1976), 54–60.

[35] Mitsuru Nakajima, Keisuke Hasegawa, Yasutoshi Makino, and Hiroyuki Shinoda. 2018. Remotely displaying cooling sensation via ultrasound-driven air flow. In *2018 IEEE Haptics Symposium (HAPTICS)*. IEEE, 340–343.

[36] Mitsuru Nakajima, Keisuke Hasegawa, Yasutoshi Makino, and Hiroyuki Shinoda. 2021. Spatiotemporal Pinpoint Cooling Sensation Produced by Ultrasound-Driven Mist Vaporization on Skin. *IEEE Transactions on Haptics* (2021).

[37] Arinobu Niijima, Toki Takeda, Takafumi Mukouchi, and Takashi Satou. 2020. Thermalbitdisplay: Haptic display providing thermal feedback perceived differently depending on body parts. In *Extended Abstracts of the 2020 CHI Conference on Human Factors in Computing Systems*. 1–8.

[38] Roshan Lalintha Peiris, Liwei Chan, and Kouta Minamizawa. 2016. Thermocons: Evaluating the thermal haptic perception of the forehead. In *Proceedings of the 29th Annual Symposium on User Interface Software and Technology*. 187–188.

[39] Roshan Lalintha Peiris, Wei Peng, Zikun Chen, Liwei Chan, and Kouta Minamizawa. 2017. Thermovr: Exploring integrated thermal haptic feedback with head mounted displays. In *Proceedings of the 2017 CHI Conference on Human Factors in Computing Systems*. 5452–5456.

[40] John I. Hochstein Philip M. Gerhart, Andrew L. Gerhart. 2015. *Munson, Young and Okiishi's Fundamentals of Fluid Mechanics*. Wiley.

[41] Nicolaas Prins et al. 2016. *Psychophysics: a practical introduction*. Academic Press.

[42] Nimesha Ranasinghe, Pravar Jain, Shienny Karwita, David Tolley, and Ellen Yi-Luen Do. 2017. Ambiotherm: enhancing sense of presence in virtual reality by simulating real-world environmental conditions. In *Proceedings of the 2017 CHI Conference on Human Factors in Computing Systems*. 1731–1742.

[43] Ahsan Raza, Waseem Hassan, Tatyana Ogay, Inwook Hwang, and Seokhee Jeon. 2019. Perceptually correct haptic rendering in mid-air using ultrasound phased array. *IEEE Transactions on Industrial Electronics* 67, 1 (2019), 736–745.

[44] Thijs Roumen, Simon T Perrault, and Shengdong Zhao. 2015. Notiring: A comparative study of notification channels for wearable interactive rings. In *Proceedings of the 33rd Annual ACM Conference on Human Factors in Computing Systems*. 2497–2500.

[45] Satoshi Saga. 2015. HeatHapt thermal radiation-based haptic display. In *Haptic Interaction*. Springer, 105–107.

[46] Emily Shaw, Tessa Roper, Tommy Nilsson, Glyn Lawson, Sue VG Cobb, and Daniel Miller. 2019. The heat is on: Exploring user behaviour in a multisensory virtual environment for fire evacuation. In *Proceedings of the 2019 CHI Conference on Human Factors in Computing Systems*. 1–13.

[47] Anshul Singhal and Lynette A Jones. 2015. Dimensionality of thermal icons. In *2015 IEEE World Haptics Conference (WHC)*. IEEE, 469–474.

[48] Anshul Singhal and Lynette A Jones. 2017. Perceptual interactions in thermotactile displays. In *2017 IEEE World Haptics Conference (WHC)*. IEEE, 90–95.

[49] Joseph C Stevens. 1982. Temperature can sharpen tactile acuity. *Perception & psychophysics* 31, 6 (1982), 577–580.

[50] Joseph C Stevens. 1989. Temperature and the two-point threshold. *Somatosensory & motor research* 6, 3 (1989), 275–284.

[51] Joseph C Stevens and Barry G Green. 1978. Temperature–touch interaction: Weber's phenomenon revisited. *Sensory processes* (1978).

[52] I A et al. Strigo. 2000. Effect of ambient temperature on human pain and temperature perception. *Anesthesiology* 92,3 (2000), 699–707.

[53] Ryoko Takahashi, Keisuke Hasegawa, and Hiroyuki Shinoda. 2018. Lateral modulation of midair ultrasound focus for intensified vibrotactile stimuli. In *International Conference on Human Haptic Sensing and Touch Enabled Computer Applications*. Springer, 276–288.

[54] Ryoko Takahashi, Keisuke Hasegawa, and Hiroyuki Shinoda. 2019. Tactile stimulation by repetitive lateral movement of midair ultrasound focus. *IEEE transactions on haptics* 13, 2 (2019), 334–342.

[55] Peter Weir, Christian Sandor, Matt Swoboda, Thanh Nguyen, Ulrich Eck, Gerhard Reitmayr, and Arindam Day. 2013. *Burnar: Involuntary heat sensations in augmented reality*. IEEE.

[56] Reto Wettach, Christian Behrens, Adam Danielsson, and Thomas Ness. 2007. A thermal information display for mobile applications. In *Proceedings of the 9th international conference on Human computer interaction with mobile devices and services*. 182–185.

[57] Graham Wilson, Stephen Brewster, Martin Halvey, and Stephen Hughes. 2012. Thermal icons: evaluating structured thermal feedback for mobile interaction. In *Proceedings of the 14th international conference on Human-computer interaction with mobile devices and services*. 309–312.

[58] Jiayi Xu, Yoshihiro Kuroda, Shunsuke Yoshimoto, and Osamu Oshiro. 2019. Non-contact cold thermal display by controlling low-temperature air flow generated with vortex tube. In *2019 IEEE World Haptics Conference (WHC)*. IEEE, 133–138.

[59] Gi-Hun Yang, Ki-Uk Kyung, Mandayam A Srinivasan, and Dong-Soo Kwon. 2006. Quantitative tactile display device with pin-array type tactile feedback and thermal feedback. In *Proceedings 2006 IEEE International Conference on Robotics and Automation, 2006. ICRA 2006*. IEEE, 3917–3922.

[60] Tae-Heon Yang, Jin Ryong Kim, Hanbit Jin, Hyunjae Gil, Jeong-Hoi Koo, and Hye Jin Kim. 2021. Recent Advances and Opportunities of Active Materials for Haptic Technologies in Virtual and Augmented Reality. *Advanced Functional Materials* (2021), 2008831.

[61] David Yarnitsky and Elliot Sprecher. 1994. Thermal testing: normative data and repeatability for various test algorithms. *Journal of the neurological sciences* 125, 1 (1994), 39–45.

[62] David Yarnitsky, Elhor Sprecher, Ruth Zaslansky, and Jeshayachu A. Hemli. 1995. Heat pain thresholds: normative data and repeatability. *Pain* 60, 3 (1995), 329–332. https://doi.org/10.1016/0304-3959(94)00132-X

[63] Kazuma Yoshino and Hiroyuki Shinoda. 2014. Contactless touch interface supporting blind touch interaction by aerial tactile stimulation. In *2014 IEEE Haptics Symposium (HAPTICS)*. IEEE, 347–350.